

TEACHING SHUNT FACTS DEVICES WITH THE EMTP

P.G. Barbosa, A.C.S. de Lima, E.H. Watanabe and S. Carneiro Jr.

COPPE - Federal University of Rio de Janeiro
 Department of Electrical Engineering
 P.O. Box 68504
 21945-970 Rio de Janeiro - RJ
 email: pedro@coe.ufrj.br or siqueira@coe.ufrj.br

Abstract - This paper deals with the modeling of shunt FACTS devices based on thyristors and self-commutated switches (GTO, IGBT, etc.). In this sense, thyristor based shunt and advanced shunt compensators are presented. Following each compensator model some computer simulation and laboratory scale experimental results will be presented and discussed.

I. INTRODUCTION

THE era of FACTS devices can be said to have begun with the pioneering work of Hingorani in 1988 [1]. In that paper, Hingorani proposes the extensive use of Power Electronics, or as he calls: Mega-Watt Electronics, for the control of AC power systems. His basic idea was to obtain AC power systems with high level of operational flexibility similar to that achieved with HVDC systems. These ideas were based on the use of thyristor, as well as on the development of the new self-commutated (controllable turn-on and turn-off) semi-conductor devices like GTO (Gate Turn-off Thyristor), MCT (MOS Controlled Thyristor) and IGBT (Insulated Gate Bipolar Transistor) [2].

The technology for connecting thyristors in series (in some cases more than 100) is well known and important for high power applications. Today the maximum breakdown voltage and current conduction capabilities for thyristors are around 8 kV and 4 kA, respectively. However, the switching characteristic of thyristors is appropriate for using in line-commutated converters, like in HVDC systems.. These are the main aspects that make thyristors very adequate for FACTS applications.

The other new devices, mentioned above, are self-commutated and appropriate for use in force-commutated converters. At the present, GTO is the main options for high power converters design. However, the series connection of these devices is a relatively complicated problem. The actual technology allows the connection of few switches in series. Thus, high power converters are normally achieved by the use of several converters with few series switches.

An increasing importance of FACTS devices in power utilities cannot be neglected. Thus, graduate and undergraduate curricula must be updated with this subject. As a contribution to this problem some EMTP simulation will be presented to show the basic operating principles of the shunt FACTS devices, specially those based on self-controlled semiconductors.

II. IDEAL SHUNT COMPENSATOR

Figure 1 shows a simple ac system composed by two ideal machines and a short transmission line without losses. A

continuously controlled voltage source was shunt connected in the middle of the transmission line with the objective of controlling its power flow. For this analysis it will be assumed that the voltages V_S and V_R (*bold typed letters are phasors*) have the same magnitude and are phase-shifted by δ .

Figure 2 shows the phasor diagram of the system for the case when the compensation voltage V_M has the same magnitude, as V_S and V_R . In this case, the active power transferred from V_S to the load side V_R is given by:

$$P_S = \frac{2V^2}{X_L} \sin(\delta/2), \quad (1)$$

where V is the magnitude of the voltages V_S and V_R .

If no compensation were present this power would be given by:

$$P_S = \frac{V^2}{X_L} \sin \delta. \quad (2)$$

Therefore, comparing (1) and (2), it is clear that the shunt reactive power compensation improves the power transfer capability of the line [4]. From Fig. 2 is also possible to conclude that, since the compensation current I_M is in quadrature with the voltage V_M , there is no active power flowing through this source. That is, only reactive power flows through the source V_M . This is an important conclusion because it will make the synthesis of this "source" easier.

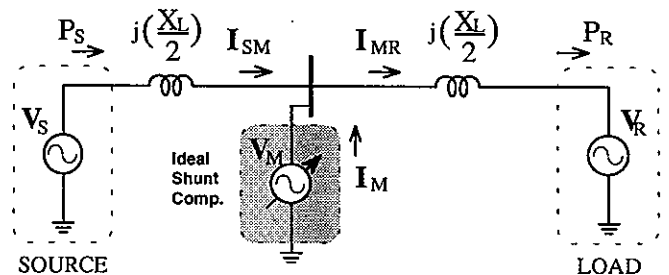


Figure 1: Ideal shunt compensator connected in the middle of a transmission line.

Figure 3 shows the steady-state active power transfer capability of the ac systems with and without the shunt compensation. Note that the shunt compensator increases the system dynamic stability margin.

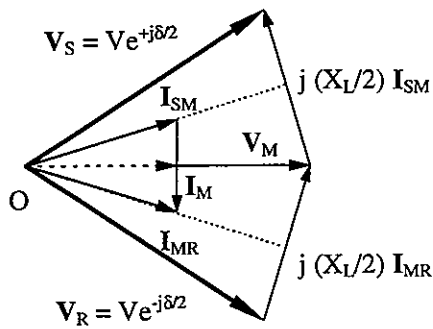


Figure 2: Phasor diagram of the system with shunt reactive power compensation.

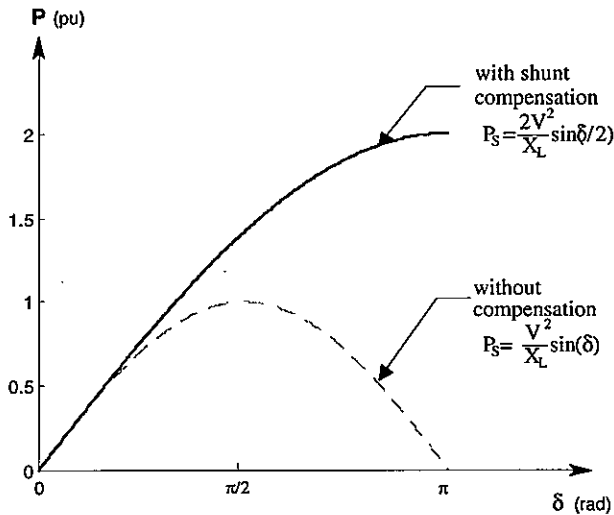


Figure 3: Power transfer characteristics for the case of shunt compensation and no-compensation.

III. STATIC VAR COMPENSATORS (SVC)

Figure 4 (a) shows the basic Thyristor Controlled Reactor (TCR). The use of a phase control produces an equivalent continuous variable inductance at TCR terminals. However, due to the switching operation, low order harmonic currents will appear. Therefore, transformers with wye-delta connection and passive filters may be necessary to eliminate these harmonics.

Figure 4 (b) shows the Thyristor Switched Capacitor (TSC). In this circuit, the thyristor is turned-on only when zero voltage switching condition is achieved, which means that the voltage at the terminals of the thyristor has to be zero at the turn-on instant. Thus the capacitors can be only connected or disconnected to the grid and a step-like control all that is possible. Since the switching is done normally at very low frequency, the harmonics are not a serious concern.

The compensators shown in Fig.4 allow only capacitive or inductive compensation. However, in most of the applications, it is desirable to have continuous compensator characteristics, from capacitive to inductive and vice-versa. The Static Var Compensator (SVC) is designed to operate in this way.

Figure 5 (a) shows a single-line diagram of a SVC. In this figure, a thyristor controlled reactor is connected in parallel with a fixed or switched capacitor. The filter is not shown.

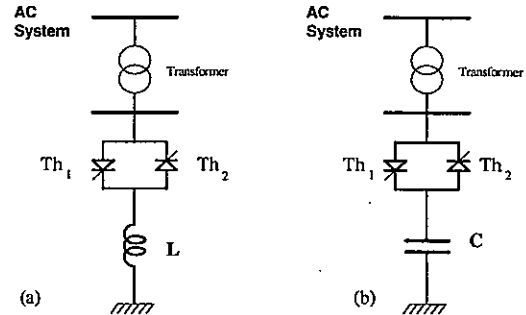


Figure 4: Thyristor based FACTS devices: (a) Thyristor controlled reactor (TCR); (b) Thyristor switched capacitor (TSC).

The capacitor C of the SVC is calculated in such a way as to generate the maximum reactive power that the compensator has to supply. This condition will happen when the thyristors are not turned-on ($\alpha=180$ degrees). On the other hand, the TCR inductor should be able to absorb the reactive power from the capacitor bank and a desired reactive power from the AC network. This will occur when the thyristors are turned-on at minimum angle ($\alpha=90$ degree). Thus, the SVC can generate or absorb controlled reactive power. In this sense, the AC network can "see" an adjustable fundamental frequency susceptance controlled by the firing angle of the TCR thyristors ($90^\circ < \alpha < 180^\circ$).

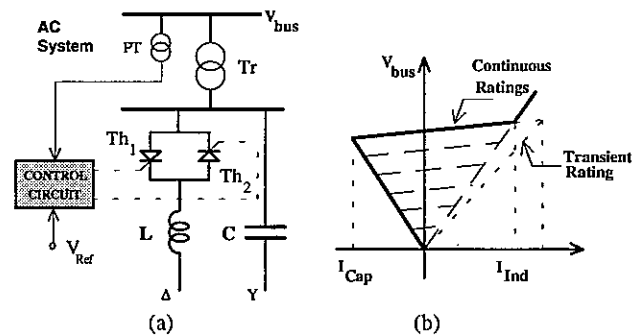


Figure 5: (a) Circuit diagram of a Static Var Compensator; (b) VxI characteristics.

Figure 6 shows a schematic diagram of the control circuit used in the above compensator. An easy way to implement the controller below is using the built-in TACS devices [11].

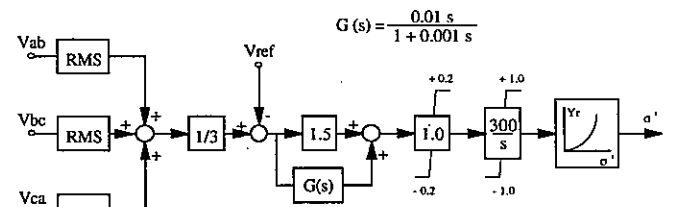


Figure 6: Schematic control block diagram of SVC.

A. Digital Simulation

Digital simulation results of the SVC are obtained with the EMTP for the system shown in Fig. 1. The ac transmission line was modeled using 2x100 km section of the distributed line model with constant parameters (Table I). The power supply was represented as 230 kV line-to-line ideal voltage source behind a transient reactance.

Table I - Transmission line parameters.

#	R (Ω /km)	L (mH/km)	C (μ F/km)
Zero seq.	0.03167	3.2220	0.00787
Pos. seq.	0.02430	0.9238	0.01260

Figure 7 shows the current flowing in one branch of the TCR. The objective here was to test the initialization strategy and adjust the control gains. The thyristors firing angles are kept constant and the load was chosen as RL equivalent circuit. It is noticeable that the system takes almost 40ms to reach the steady state.

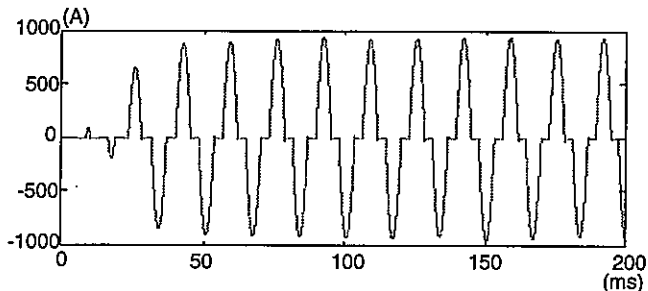


Figure 7: Initialization of TCR current in steady state.

Now we are able to test the SVC performance under sudden disturbances. In this sense, the load was modeled as an arc furnace, which is a variable step load. Fig. 8 shows the instantaneous active power flowing on the system load side. Before $t=100$ ms, the load is essentially light and the compensator goes to operate with inductive characteristic. After $t=100$ ms, the active power drained by the load increases, thus TCR is continuously reduced until the compensator reaches its maximum capacitive characteristic. Fig. 9 shows one branch TCR current. Note that it varies softly from its maximum value to zero after the step is applied in the load. Fig. 10 shows the line-to-line SVC voltage. As explained before the system takes approximately 30 ms to reach the steady state. However, after this time the systems take less than one cycle to achieve the specified condition.

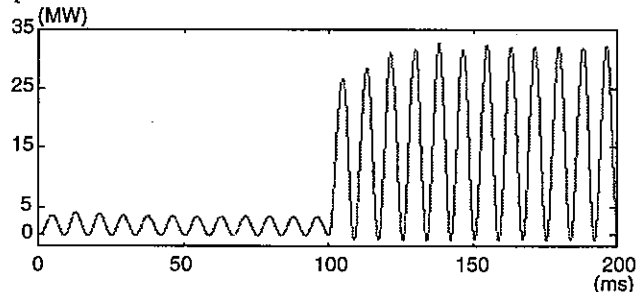


Figure 8: Instantaneous Power in the arc furnace

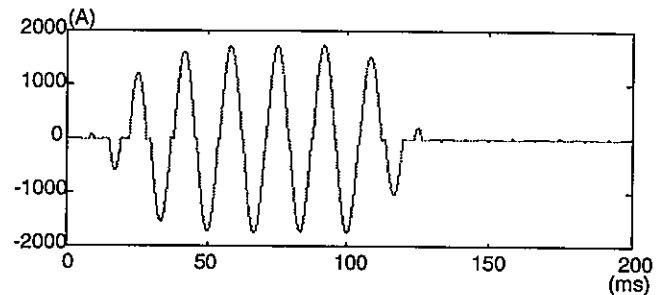


Figure 9: TCR current with an arc furnace load.

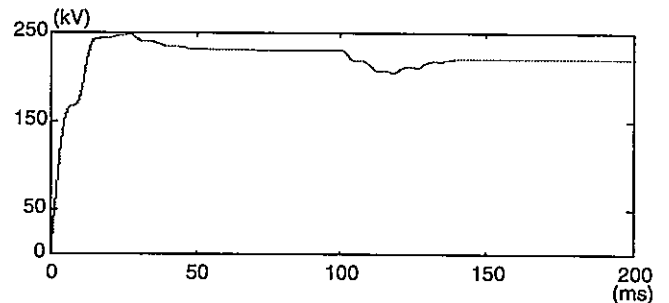


Figure 10: RMS bus voltage on the SVC connection bus.

IV. ADVANCED SHUNT VAR COMPENSATORS (ASVC)

The development of high power self-commutated devices as GTO have led to the possibility of designing high power voltage source inverters (VSI), as shown in Fig. 11. In these converters, the switches are composed by a GTO with anti-parallel connected diode. These switches operate with unidirectional voltage blocking capability and bidirectional current flow [2].

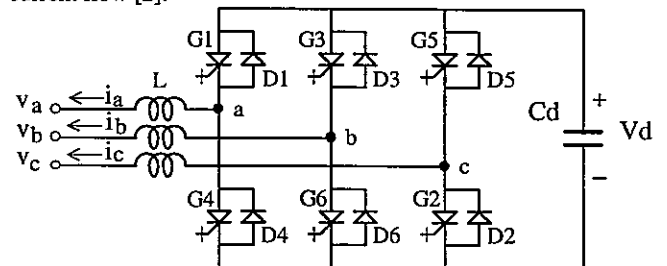


Figure 11: Voltage source inverter (VSI).

Figure 12 (a) shows a schematic single line diagram of the proposed VSI shunt connected to the ac system. The VSI and the control block, which needs the measurement of the ac voltages and line currents, is called *Advanced Shunt Var Compensator (ASVC)*. Fig. 12 (b) shows the ASVC output $V \times I$ characteristic.

In the case of shunt compensators when only reactive power has to be compensated, the DC voltage source may be replaced by a small capacitor. Nevertheless, if active power has to be absorbed by the compensator, an energy sink should be connected at the DC side of the VSI. As a first choice, the dc sink may be a resistance. However, if the power absorbed is to be returned to the ac system during the next cycles, a large energy storage system may be used.

In practical applications, small reactors (L) are used to connect the VSI to the AC network. They are necessary to avoid current peaks during switching transients. In most cases, these small reactors are just the leakage inductances of the coupling transformers.

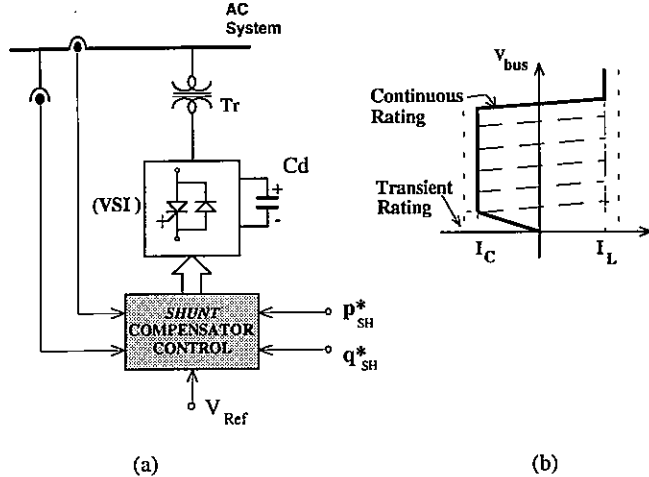


Figure 12: (a) Advanced Shunt Var Compensator based on Voltage Source Inverter; (b) output VxI characteristics.

The control algorithm of the proposed advanced shunt compensator is based on the concepts of the instantaneous $p-q$ power theory [5]. Thus, if the VSI is controlled to compensate for a given real power p_c (W) and imaginary power q_c (VAR) the shunt reference compensation currents are given in (a-b-c) coordinates by:

$$\begin{bmatrix} i_{ca}^* \\ i_{cb}^* \\ i_{cc}^* \end{bmatrix} = \sqrt{\frac{2}{3}} \begin{bmatrix} 1 & 0 \\ -\frac{1}{2} & \frac{\sqrt{3}}{2} \\ -\frac{1}{2} & -\frac{\sqrt{3}}{2} \end{bmatrix} \begin{bmatrix} v_\alpha & v_\beta \\ -v_\beta & v_\alpha \end{bmatrix}^{-1} \begin{bmatrix} p_c \\ q_c \end{bmatrix} \quad (3)$$

where the currents with superscript (*) are the references that the compensator has to synthesize.

Ideally, the proposed Advanced Shunt Compensator is designed to generate or absorb only reactive power. Thus,

$$p_c = p_{SH}^* = 0 \quad \text{and} \quad q_c = q_{SH}^* \quad (4)$$

where q_{SH}^* is the reference shunt imaginary power that has to be injected or absorbed by the compensator. Therefore, the ASVC operates as three controllable current sources connected in parallel to the ac line.

A. Digital Simulation

The performance of ASVC, with 50 MVA / 230 kV and 1000 μ F / 25 kV DC capacitor, was analyzed using the EMTP. The VSI control was based on the PWM adaptive current control and the maximum switching frequency was 8 kHz. Nowadays, the design of high frequency high power VSI is not possible yet. However, similar current waveforms that will be presented could be obtained by using multistage inverters [4] or multilevel inverters [7].

Figure 13 shows a block diagram of the control algorithm of the ASVC. The inverter output current can track their references (i_{ca}^* , i_{cb}^* and i_{cc}^*) with a very small amplitude error or phase delay. The instantaneous active power p_c is used to maintain the converter dc voltage (V_d) at a given value. The DC voltage error is fed to a PI-controller. The output of which (Δp) is added to the instantaneous active power reference signal (p_{SH}^*). The basic TACS control structure is shown in the appendix.

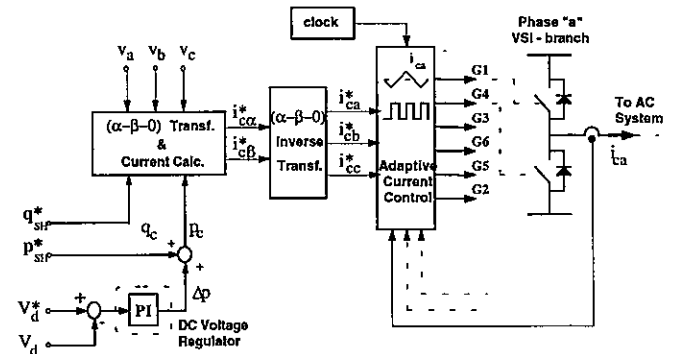


Figure 13: Control block diagram of the ASVC.

In the simulations that will be presented the ASVC was connected directly to the utility system without any special load. Fig. 14 (a) and (b) shows the system voltage and the compensator current when the reference value q_{SH}^* is step changed from zero to its maximum inductive value (+50 MVA) in $t = 20$ ms. In Fig. 15 (a) and (b), the situation is very similar, except that the reference value q_{SH}^* is step changed from zero to its maximum capacitive value (-50 MVA). The compensator response is almost instantaneous in both cases. During the time before the step is applied the currents show a small fundamental component. These currents are responsible for the DC capacitor voltage regulation. Fig. 16 shows a transient response for the case of step change in the reactive power reference from maximum inductive to maximum capacitive current in $t = 25$ ms.

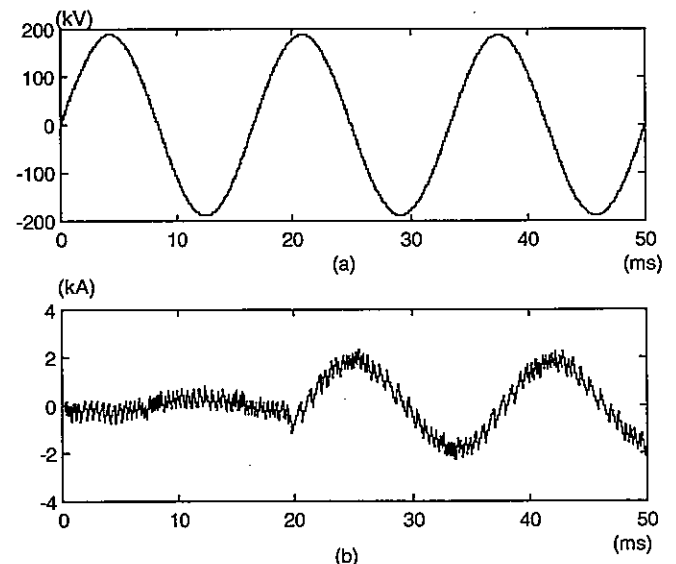


Figure 14: (a)-Phase voltage and (b)-compensator current for inductive step variation of reactive reference signal.

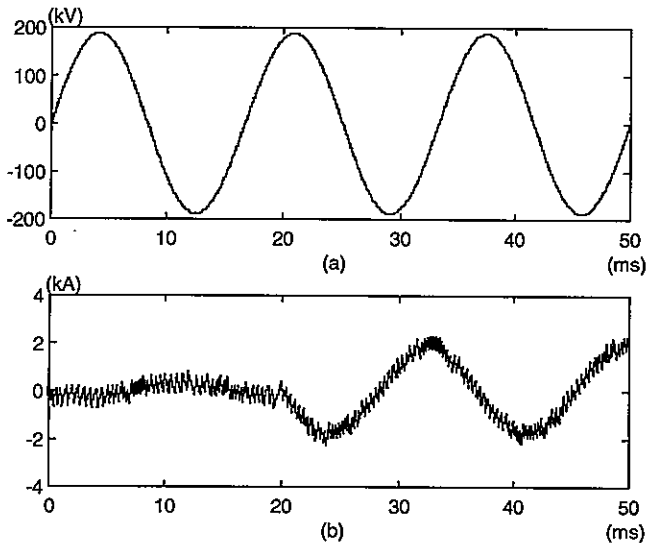


Figure 15: (a)-Phase voltage and (b)-compensator current for capacitive step variation of reactive reference signal.

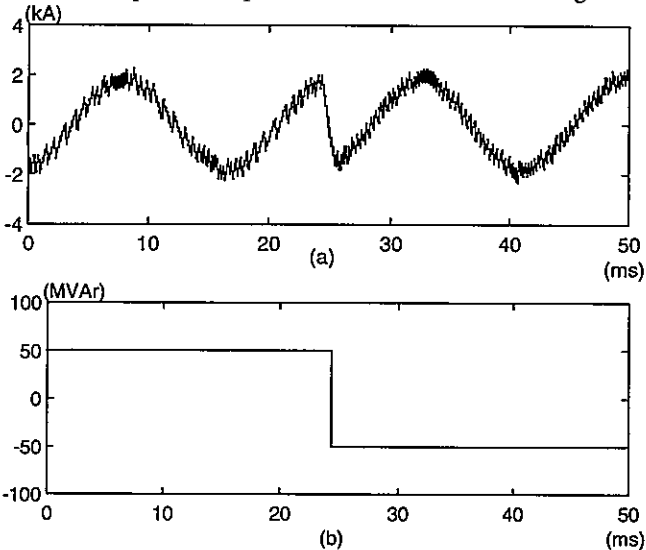


Figure 16: (a)-Compensator current and (b)-step variation of reactive reference signal from inductive to capacitive.

B. Experimental Results

A 500 VA / 55 V small laboratory prototype ASVC, with a 12 μ F / 100 V DC capacitor, was used to obtain some experimental results. The switching frequency is 7 kHz.

Figures 15 and 16 show respectively the steady state system phase voltage and compensation current for a capacitive ($q_{SH}^* < 0$) and inductive ($q_{SH}^* > 0$) characteristics. Fig. 17 shows a transient response for the case of step change in the reactive power reference from inductive to capacitive current. Note that the compensator is able to go from one extreme of reactive compensation to the other extreme in less than 1 ms, which is a very fast response. The current waveforms show some high frequency harmonics due to the switching of the semiconductor switches. Similar to the EMTP results, here no filter was used. However in practical systems some high frequency filters may be necessary to eliminate these harmonics.

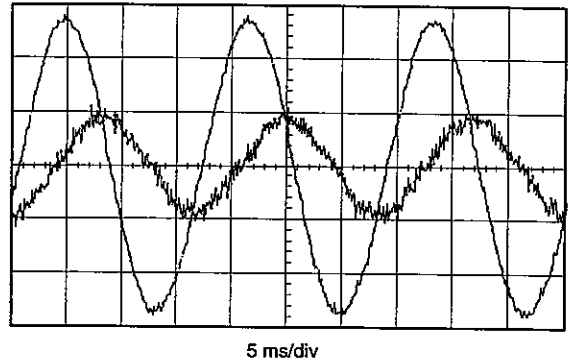


Figure 15: Experimental system phase voltage and compensator inductive current (vertical scales: 25V/div., 2A/div.).

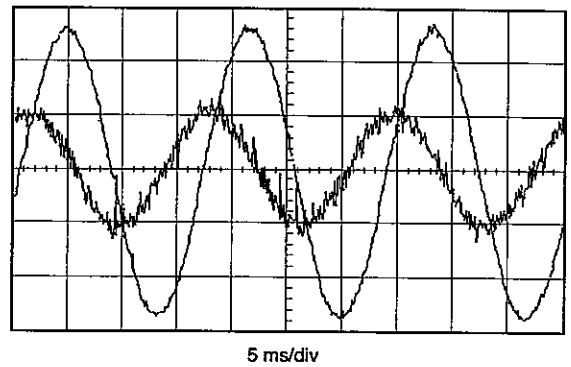


Figure 16: Experimental system phase voltage and compensator capacitive current (vertical scales: 25V/div., 2A/div.).

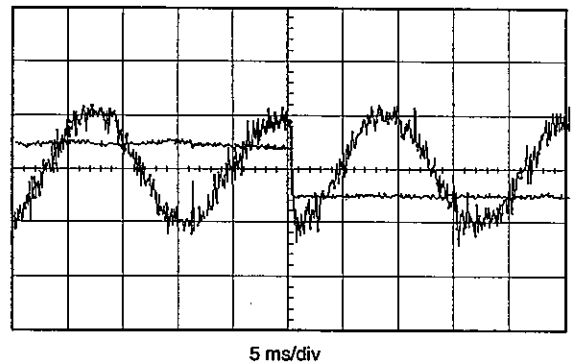


Figure 17: Experimental step response of advanced compensator (vertical scales: 2A/div. and 1kVar/div.).

VIII. CONCLUSIONS

This paper presents some basic concepts and principles of operation of shunt FACTS devices. The main objective was not to present which is the best, but just to show how they operate, their advantages, limitations and try to make them easier to understand to graduate and undergraduate students. The EMTP was used to illustrate the performance of some of these devices.

The use of thyristors and self-commutated devices was treated separately, because they lead to different configurations and control systems. The instantaneous power theory was used to design the control the ASVC. The authors are convinced that this

theory should be well understood as it will find increasing applications in the design of advanced compensators.

IX. REFERENCES

- [1] N. G. Hingorani, "Power Electronics in Electric Utilities: Role of power Electronics in Future power systems", *Proceedings of the IEEE*, Vol. 76, No. 4, April, 1988.
- [2] B. K. Bose, "power Electronics and AC Drives", Prentice-Hall, 1986.
- [3] L. Gyugyi, "Solid-state Control of AC Power Transmission", *Workshop on the Future in High-Voltage Transmission: Flexible AC Transmission Systems (FACTS)*, Cincinnati, Ohio, Nov., 1990.
- [4] S. Mori, K. Matsuno, M. Takeda, M. Seto, "Development of a Large Static Var Generator Using Self-Commutated Inverters for Improving Power System Stability", *IEEE Trans. on Power Delivery*, Vol. 8, No. 1, February 1993.
- [5] C. Schauder, M. Gernhardt, E. Stacey, T. Lemak, L. Gyugyi, T. W. Cease and A. Edris, "Development of a ± 100 Mvar Static Condenser for Voltage Control of Transmission System", *IEEE Trans. on Power Delivery*, Vol. 10, No. 3, July, 1995.
- [6] N. G. Hingorani, "Introducing Custom Power", *IEEE Spectrum*, pp. 41-48, June, 1995.
- [7] A. Iizuka et al. - "Self-commutated Static Var Generator at Shintakatsu Substation", *Proc. of International Power Electronic Conference - IPEC'95*, Yokohama, Japan, April, 1995.
- [8] H. Akagi, Y. Kanazawa and A. Nabae, "Instantaneous Reactive Power Compensators Comprising Switching Devices without Energy Storage Components", *IEEE Trans. on Ind. Appl.*, Vol. IA-20, No. 3, 1984.
- [9] E. H. Watanabe, R. M. Stephan and M. Aredes, "New Concepts of Instantaneous Active and Reactive Power for Three Phase System and Generic Loads", *IEEE Trans. on Power Delivery*, Vol. 8, No. 2, April, 1993.
- [10] P.G. Barbosa, I. Misaka and E.H. Watanabe, "Shunt-PWM Advanced Var Compensators Based on Voltage Source Inverters For FACTS Applications", *Proc. of 4th Symposium of Specialists in Electric Operational and Expansion Planning - IV SEPOPE*, SP-11, Foz do Iguacu, Brazil, May, 1994.
- [11] A.C.S. de Lima, R.M. Stephan and S. Wanderley, "Modelling a Static Var Compensator Using EMTP", *Proc. of the 38th MWSCAS*, Rio de Janeiro, June, 1995.

APPENDIX

TACS template for ASVC model

```

##### GENERAL TACS SOURCES
90E_A
90E_B
90E_C
91IC_A
91IC_B
91IC_C
C ##### PWM MODULATION CLOCK (8kHz)
23CLOCK 10. 1.25E-04 6.25E-05 -f.
C ##### ALFA-BETA TRANSFORMATION & CURRENT CALCULATION
99VALFA = SQRT(2/3)*(E_A -5*E_B -5*E_C )
99VBETA = SQRT(2/3)*(E_B -E_C )/2
99PSH = 0 + D_P
99QSH = 5.0E07
99IALFAC = (VALFA*PSH+VBETA*QSH)/( VALFA*VALFA+VBETA*VBETA )
99IBETAC = (VBETA*PSH-VALFA*QSH)/( VALFA*VALFA+VBETA*VBETA )
C ##### INVERSE ALFA-BETA TRANSFORMATION
99IAREF = SQRT(2/3)*IALFAC
99IBREF = SQRT(2/3)*(-.5*IALFAC+SQRT(3)*IBETAC/2)
99ICREF = SQRT(2/3)*(-.5*IALFAC-SQRT(3)*IBETAC/2)
C ##### ADPTIVE CURRENT CONTROL & GATE SIGNAL (PHASE A)
98ERR_A 60 ZERO +UNITY +UNITY IC_A IAREF
98G_1 62+ERR_A CLOCK
98G_4 =NOT.(G_1)

```